

Impacts of Integrating Topology Reconfiguration and Vehicle-to-Grid Technologies on Distribution System Operation

Zhaomiao Guo, Zhi Zhou, *Member, IEEE*, and Yan Zhou

Abstract—Autonomous electric vehicles (AEVs) provide unique opportunities to cope with the uncertainties of distributed energy generation in distribution networks. But the effects are limited by both inherent radial topology and the behaviors of decentralized AEVs. We investigate the potential benefits of dynamic distribution network reconfiguration (DDNR), taking into account AEVs' spatial-temporal availability and their charging demand. We propose a mixed integer programming model to optimally coordinate the charging/discharging of AEVs with DDNR, while satisfying AEVs' original travel plan. Numerical studies based on a test system overlaying the IEEE 33-node test feeder and Sioux Falls transportation network show that DDNR and AEV complement each other, which improves the operation of distribution system. We also conduct sensitivity analyses on inputs including renewable fluctuation and AEVs penetration level.

Index Terms—distribution network reconfiguration (DNR), urban transportation network, autonomous electric vehicle (AEV), controllable charging, vehicle-to-grid (V2G).

NOMENCLATURE

Sets and Indices

- \mathcal{N} : set of power distribution nodes, indexed by m or n , $N = |\mathcal{N}|$
 - \mathcal{N}^l : set of load nodes
 - \mathcal{N}^s : set of substation nodes
- \mathcal{E} : set of distribution lines, indexed by nm , where n is the from node and m is the to node, $E = |\mathcal{E}|$
 - \mathcal{E}^s : set of lines equipped with RCSs
- \mathcal{T} : set of time periods, indexed by t , $T = |\mathcal{T}|$
- \mathcal{V}_n : set of EVs at bus n , indexed by v , $V_n = |\mathcal{V}_n|$
- \mathcal{R} : set of trip destinations, indexed by r
- \mathcal{S} : set of candidate charging locations, indexed by s
- \mathcal{N}' : set of transportation nodes, indexed by n'
- \mathcal{E}' : set of transportation links, indexed by a

Parameters

- ΔT : duration of time in one period
- R_{mn} : resistance of the line mn in p.u.
- X_{mn} : Reactance of the line mn in p.u.
- C^e : unit cost of energy loss
- C^{sw} : switching cost per switching action
- $P_{n,t}^l, Q_{n,t}^l$: real and reactive load at node n in period t
- $F(\cdot)$: function of $\tan(\cos^{-1}(\cdot))$

Z. Guo is with the Department of Civil, Environmental and Construction Engineering, University of Central Florida, Orlando, FL 32816, USA

Z. Zhou (zzhou@anl.gov, corresponding author) and Y. Zhou are with the Energy Systems Division, Argonne National Laboratory, Lemont, IL 60439, USA.

- PF_v^{chg}, PF_v^{dsg} : charging/discharging power factor
- $P_{nm}^{\max}, Q_{nm}^{\max}$: maximum allowed real and reactive power flow at line nm
- $P_e^{\max,cha}, P_e^{\max,dsg}$: maximum charging/discharging rate
- $P_{n,t}^s, Q_{n,t}^s$: real and reactive power flow from substation at node n in period t
- X_{nm} : initial status of line nm : 1 closed; 0 open
- ΔX^{\max} : maximum switching actions allowed
- V^{\min}, V^{\max} : min/max of voltage
- η_v^{chg} : charging efficiency factor
- $T_v^{\text{arr}}, T_v^{\text{dep}}$: arrival and departure time of EV v
- $SOC_v^{\min}, SOC_v^{\max}$: min/max state of charge of EV v
- $SOC_v^{\text{arr}}, SOC_v^{\text{dep}}$: arrival and minimum required departure state of charge of EV v
- $z_{v,t} \in \{0, 1\}$: binary variables indicating whether v is connected to grid at time t
- ζ_v : slope of capacity degradation curve of EV v
- cap_v^{end} : normalized capacity at the end of life of EV v
- cap_v : total battery capacity of EV v
- $cap_{v,t}^{\text{loss}}$: capacity degradation of EV v at time period t
- C_v^{rep} : replacement cost of the battery of EV v
- C_v^{res} : residual value of the battery of EV v when it is at the end of life
- $d_{v,t}^{\text{shelf}}$: shelf degradation of EV v during t
- $d_{v,t}^{\text{cycle}}$: battery degradation of EV v due to charging and discharging during t
- $d_{v,t}$: actual battery degradation of EV v during t
- $c_{v,t}^{\text{deg}}$: degradation cost of EV v during t
- β_i : AEV's utility coefficients
- d^r : total travel demand from r
- A : node-link incidence matrix of transportation network
- E^{rs} : OD incidence vector of OD pair rs with +1 at origin and -1 at destination

Variables

- $x_{nm,t} \in \{0, 1\}$: lines connection status
- $z_{nm,t} \in \{0, 1\}$: lines switching action
- $y_{nm,t} \in \{0, 1\}$: binary variables indicating whether n is the parent node of m : 1 true; 0 false
- $p_{nm,t}, q_{nm,t}$: real/reactive power flow of line nm at t
- $p_{v,t}^{chg}, p_{v,t}^{dsg}, q_{v,t}^{chg}, q_{v,t}^{dsg}$: real and reactive power flow of charging and discharging of EV v in period t
- $soc_{v,t}$: state of charge of EV v in period t
- $v_{n,t}^2$: squared voltage magnitude at bus n in period t
- tt^{rs}, ts^{rs} : travel time/speed between r and s
- ρ^s : charging & parking price at s

- 1 • f_a^{rs} : link traffic flow on link a that travels from r to s
- 2 • q^{rs} : travel demand from r to s
- 3 • τ_n^{rs} : dual variable of flow (from r to s) conservation at
4 n'

5 I. INTRODUCTION

6 A UTONOMOUS electric vehicles (AEVs), such as the
 7 Tesla Autopilot [1], bring evolutionary changes to the
 8 transportation sector in terms of both mobility and energy con-
 9 sumption through influencing when, where, and how people
 10 travel. They also provide a great opportunity for efficiently
 11 and robustly operating the power network to cope with the
 12 challenges brought on by various demands and renewable
 13 generation.

14 Moreover, AEVs increase the interdependence between
 15 transportation and power networks. On one hand, charging
 16 costs and electricity availability will impact the travel be-
 17 haviors of AEVs; on the other hand, the travel behaviors of
 18 AEVs will impact the spatial and temporal distribution of
 19 energy demand as well as vehicle-to-grid (V2G) availability.
 20 Modeling this close coupling is critical to understanding the
 21 impacts of AEVs on the whole systems.

22 Compared with conventional electric vehicles (EVs), AEVs
 23 have larger flexibility on where and when to charge and
 24 park. EVs without automation are mostly charged at home
 25 or the work place[2], where travelers have relatively long
 26 dwelling time, due to the requirements of human operations for
 27 vehicle relocation. Although the deployment of public direct
 28 current (DC) fast chargers could significantly reduce charging
 29 duration, the benefits of EVs to the power system are limited
 30 because their energy flexibility is constrained by the implied
 31 logic that people using fast chargers desire to charge their
 32 vehicles as quickly as possible. Unlike EVs, the self-driving
 33 feature of AEVs enables the vehicles to travel to charging
 34 stations without intervention after arriving at a destination and
 35 maintain grid connectivity thereafter until the departure time
 36 of the next trip.

37 Despite various studies on autonomous vehicles (AVs) from
 38 various perspectives, such as ride sharing [3], obstacle detec-
 39 tion (e.g., [4]), motion control (e.g., [5]), collective behavior
 40 (e.g., [6]), and hardware technologies (e.g., [7]), the potential
 41 values of AEVs on power grid has not been as thoroughly in-
 42 vestigated. Reference [8] investigates the coordinated parking
 43 problem (CPP) of AEVs to support V2G services, assuming
 44 that AEVs can be centrally coordinated. This assumption
 45 is justifiable for a company-owned AEV fleet, but is less
 46 likely to hold for personally owned AEVs in the foreseeable
 47 future. Reference [9] models the probabilistic load flow of a
 48 residential distribution network by capturing charging voltage
 49 dependencies. It also incorporates the provision of reactive
 50 power from EVs to reduce the probability of power quality
 51 violation. Reference [10] includes a discussion on electric ve-
 52 hicles participating in frequency regulation on the power grid.
 53 Among the literature studying the value of AEVs on power
 54 grid operations, e.g. references [8], [9], [10], AEVs' travel
 55 and charging behaviors are largely overlooked. In this paper,
 56 we focus on the economic impacts of AEVs on distribution

5 network operations considering their charging location choices
 6 and travel routing.

7 The impacts of AEVs on total system cost reduction could
 8 be limited in distribution network in current settings due
 9 to several possible reasons: (1) the inherent radial topology
 10 of distribution network requires that the power stored in
 11 AEVs can only be supplied to certain downstream nodes;
 12 and (2) even reverse flow is allowed, total flow passing
 13 through feeders will increase due to V2G services. Distribution
 14 network reconfiguration (DNR) technologies have the potential
 15 to mitigate these drawbacks due to its capability of alternating
 16 flow path by changing the connectivity of distribution lines
 17 while maintaining a radial network topology. In addition, DNR
 18 is known to be capable of loss reduction, load balancing [11],
 19 and better accommodation on distributed energy resources
 20 [12]. Enabled by remote-controlled switches (RCSs), DNR can
 21 be classified into static and dynamic reconfigurations. Static
 22 reconfiguration allows both manual and RCSs to configure
 23 the network topology over a relatively longer time frame,
 24 such as yearly, seasonal, or monthly. It has been extensively
 25 studied and applied in power loss minimization [13], electric
 26 service restoration [14], voltage deviation management [15],
 27 and supply capability improvement [16], as well as for other
 28 purposes. In contrast, dynamic DNR operates RCSs in real
 29 time to reconfigure the distribution network. Reference [17]
 30 compares the loss reduction through hourly reconfiguration
 31 with several simpler topology management methods based on
 32 real networks. In coordination with reactive power control,
 33 hourly reconfiguration is utilized to minimize comprehensive
 34 cost in [18]. References [19], [20], and [21] apply dynamic
 35 reconfiguration is applied in the context of renewable energy
 36 integration. Specifically, distributed generation curtailment is
 37 minimized in [21], while reference [20] maximizes the hosting
 38 capability of distributed generation resources and reference
 39 [19] minimizes daily network losses.

40 We investigate the potential impacts of DDNR on the dis-
 41 tribution feeder with the AEV integration, taking into account
 42 AEVs' daily travel patterns, battery degradation costs and
 43 decentralized behaviors. The main contribution of this paper
 44 is three-fold: (1) we model the decentralized travel behaviors
 45 of AEVs (i.e., each AEV decides which charging location to
 46 go and which route to take in order to maximize its own
 47 utility), whose interactions form the transportation network
 48 equilibrium; (2) we explicitly connect the traffic pattern with
 49 the spatial-temporal distribution of electricity demand; and
 50 (3) we investigate the benefits of coordinating AEVs with
 51 DDNR in a distribution system. To make a clear distinction
 52 from a previous study [22], we have made the following
 53 four improvements: (1) we present a more comprehensive
 54 numerical study with rigorous analyses; (2) we added more
 55 realistic constraints, such as power quality constraints; (3) we
 56 model and analyze the impacts of AEVs and DDNR on a
 57 system with distributed renewable energy, and (4) we introduce
 58 a traffic distribution and assignment model to predict the
 59 spatial-temporal availability of AEVs. The adding transporta-
 60 tion model provides a basic framework for incentive design
 61 from a utility perspective so that utility companies can try to
 62 guide the traveling and charging behaviors of AEVs through

1 charging incentives in order to maximize the overall benefits.
 2 The remainder of this paper is organized as follows. In
 3 Section II, we introduce the mathematical formulation of the
 4 DDNR problem, travel and charging behaviors of AEVs, and
 5 battery degradation. Numerical experiments on a test system
 6 overlaying the IEEE 33-node test feeder and Sioux Falls
 7 transportation network are presented in Section III, where we
 8 compare the impacts of different technologies' availability,
 9 charging behavior assumptions, renewable output fluctuations,
 10 and AEV penetration levels on system cost and reconfiguration
 11 frequency. Finally, we conclude in Section IV with a summary
 12 of our results, contributions, and future extensions.

II. MATHEMATICAL MODELING

14 Figure 1 provides an overview of our modeling framework.
 15 Based on the charging cost and travel demand forecast each
 16 hour, drivers will select their charging/parking locations, which
 17 will determine the locational charging demand and plug-in
 18 duration. A distribution system operator (DSO) will use this
 19 information to make decisions on the day-ahead planning of
 20 the distribution network reconfiguration and optimal hourly
 21 charging/discharging plan. In this section, we first present
 22 the building components of our model, including distribution
 23 network reconfiguration, travel behaviors of AEVs, and AEVs
 24 charging and battery degradation. We integrate these com-
 25 ponents to investigate the optimal strategies for coordinating
 26 DDNR with AEVs charging in order to maximize power
 27 system benefits.

A. Distribution Network Reconfiguration Models

The baseline DDNR model is presented in (1). We consider an operation horizon of $|\mathcal{T}|$ time steps (e.g., 24 hours) and assume that feeders equipped with RCS can be controlled (with penalty) every time step, but the control scheme must be determined the day before. The objective function (1a) is to minimize the total line loss cost plus the switching cost. The original non-convex loss function $R_{nm} \cdot (p_{nm,t}^2 + q_{nm,t}^2)/v_{n,t}^2$ is simplified to $R_{nm} \cdot (p_{nm,t}^2 + q_{nm,t}^2)$, due to the assumption $v_{n,t} \approx 1.0$ pu. The same simplification is adopted in [23] and [24] when studying DNR with renewable energy resources. For a DNR problem with an objective of loss minimization, our simplification sacrifices tolerable accuracy while significantly improving the computational efficiency for the same test system compared with second order conic programming (SOCP) formulation [25]. Constraints (1b ~ 1e)¹ guarantee flow conservation for both substation and non-substation nodes; constraints (1f and 1g) limit the power flow direction based on direction indicator variables $y_{nm,t}$; constraints (1h ~ 1i) describe the voltage transition along the line, and we introduce a “big-M” method to linearize the bi-linear term; constraints (1j ~ 1k) guarantee the acceptable voltage range; constraints (1l ~ 1n) are radiality constraints; and constraint (1o) requires that the total switching actions cannot exceed a predefined limit ΔX^{\max} .

$$\min_{\mathbf{x}, \mathbf{y}, \mathbf{p}, \mathbf{q}} \sum_{t \in \mathcal{T}} \sum_{nm \in \mathcal{E}} [\Delta T \cdot R_{nm} \cdot (p_{nm,t}^2 + q_{nm,t}^2) \cdot C^e]$$

¹Throughout this manuscript, the slash operator, when applied to sets, means set subtraction.

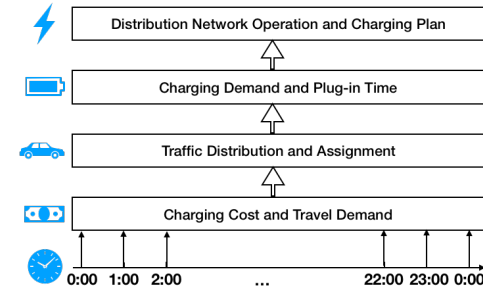


Fig. 1. Model Overview

$$+ z_{nm,t} \cdot C^{sw}] \quad (1a)$$

s.t.

$$\sum_{mn \in \mathcal{E}} p_{mn,t} = P_{n,t}^l, \forall n \in \mathcal{N}/\mathcal{N}^s, t \quad (1b)$$

$$\sum_{mn \in \mathcal{E}} q_{mn,t} = Q_{n,t}^l, \forall n \in \mathcal{N}/\mathcal{N}^s, t \quad (1c)$$

$$P_{n,t}^s = \sum_{m:mn \in \mathcal{E}} p_{nm,t}, \forall n \in \mathcal{N}^s, t \quad (1d)$$

$$Q_{n,t}^s = \sum_{m:mn \in \mathcal{E}} q_{nm,t}, \forall n \in \mathcal{N}^s, t \quad (1e)$$

$$-x_{nm,t} P_{nm}^{\max} \leq p_{nm,t} \leq x_{nm,t} P_{nm}^{\max}, \forall nm, t \quad (1f)$$

$$-x_{nm,t} Q_{nm}^{\max} \leq q_{nm,t} \leq x_{nm,t} Q_{nm}^{\max}, \forall nm, t \quad (1g)$$

$$\nu_{n,t}^2 \leq \nu_{m,t}^2 - 2(R_{nm} p_{mn,t} + \chi_{nm} q_{mn,t}) + M(1 - x_{mn,t}), \quad \forall mn, t \quad (1h)$$

$$\nu_{n,t}^2 \geq \nu_{m,t}^2 - 2(R_{nm} p_{mn,t} + \chi_{nm} q_{mn,t}) - M(1 - x_{mn,t}), \quad \forall mn, t \quad (1i)$$

$$\nu_{n,t}^2 = 1 \text{ p.u.}, \forall n \in \mathcal{N}^s, t \quad (1j)$$

$$V^{\min} \leq \nu_{n,t} \leq V^{\max}, \forall n \in \mathcal{N}/\mathcal{N}^s, t \quad (1k)$$

$$y_{mn,t} = 0, \forall n \in \mathcal{N}^s, mn, t \quad (1l)$$

$$\sum_{m:mn \in \mathcal{E}} y_{mn,t} = 1, \forall n \in \mathcal{N} \setminus \mathcal{N}^s \quad (1m)$$

$$y_{nm,t} + y_{mn,t} = x_{nm,t}, \forall nm \quad (1n)$$

$$\sum_{t \in \mathcal{T} \setminus \{0\}} \sum_{nm \in \mathcal{E}} (x_{nm,t} - x_{nm,t-1})^2 \leq \Delta X^{\max} \quad (1o)$$

1
2
3
4
5

Notice that since we focus on the potential impacts of coordinating AEVs charging/discharging with DDNR, we incorporate intermittent renewable generation as net load from the modeling perspective.

As shown in [25], $y_{nm,t}$ can be relaxed to continuous variables, while still maintaining the radial configuration. We adopt this relaxation in our computation to reduce the number of integer variables. In addition, we can reformulate constraint (1o) as (2) so that DDNR problem (1) is a standard mixed integer QP with a polyhedral feasible set.

$$x_{nm,t} - x_{nm,t-1} \leq z_{nm,t}, \forall nm, t \in \mathcal{T} \setminus \{0\} \quad (2a)$$

$$x_{nm,t-1} - x_{nm,t} \leq z_{nm,t}, \forall nm, t \in \mathcal{T} \setminus \{0\} \quad (2b)$$

$$\sum_{t \in \mathcal{T} \setminus \{0\}} \sum_{nm \in \mathcal{E}} z_{nm,t} \leq \Delta X^{\max} \quad (2c)$$

1 B. Travel Behaviors of AEVs in Transportation Network

2 In this subsection, we develop a model to quantify the
 3 aggregated energy availability and charging demand from
 4 AEVs in traffic equilibrium considering their travel plan and
 5 individual utility.

6 Privately owned AEVs are decentralized; in other words,
 7 each AEV makes location and route choices in order to maxi-
 8 mize its individual utility. In contrast to conventional vehicles,
 9 AEVs have the flexibility to decide where to park and charge,
 10 especially for those destinations with long dwelling times
 11 (such as home or workplace), as long as they have sufficient
 12 battery for the next trip before the scheduled departure time.
 13 We adopt a multinomial logit model, which is an extension
 14 of logistic regression to multiclass problems [26], to describe
 15 the choice of different charging location s from last trip's
 16 destination r (e.g., home or workplace), with the deterministic
 17 component of utility function as follows:

$$U^{rs} = \beta_0^s - \beta_1 tt^{rs} - \beta_2 \rho^s \quad (3)$$

18 We assume that the utility function of AEVs from node r
 19 to node s is the summation of three parts (with coefficietns
 20 $\beta_0 \sim \beta_2$): locational specific attractiveness factor, travel time,
 21 and service cost. The service cost can be negative, indicating
 22 the charging provider is offering incentives to AEVs for
 23 connecting at their locations. Although service delay is not
 24 explicitly modeled in the utility function, it can be incorporated
 25 as part of the travel time by adding a dummy link representing
 26 service congestion. Alternative utility function forms can be
 27 used without affecting the modeling framework adopted in this
 28 study.

We adopt the classic combined distribution and assignment (CDA) model (see [27], and more recently [28]) to calculate the equilibrial travel time and facility selection by solving a convex optimization problem. We denote the transportation network by a directed graph $\mathcal{G}' = (\mathcal{N}', \mathcal{E}')$. The CDA model for AEVs is shown in (4). For conciseness, we omit the time index for all the parameters and variables in (4). Constraints (4b) and (4c) describe the transportation flow conservation: (4b) ensures the flow conservation at each node, including the origin and destination nodes; and (4c) restricts the total trips originated from node r to be equal to the total travel demand at that location. The objective function (4a) is constructed in order to guarantee the first Wardrop principal; in other words, the journey times in all routes used are equal and less than those that would be experienced by a single vehicle on any unused route [29] and the multinomial logit² destination choice assumption being satisfied. Notice that in formulation (4), we only consider the traffic flow of AEV trips from location r to a charging/parking facility s . The traffic flows associated with conventional vehicles can be considered as background traffic. The equilibrial travel time for each OD pair rs can be

² $q(\ln q - 1)$ is added to (4a), as well as components from utility function (3), because its first-order derivative with respective to q equals to $\ln q$, which will recover flow distribution under a multinomial logit assumption.

calculated as $tt^{rs} \doteq \tau_r^{rs} - \tau_s^{rs}$ [27], and the total number of AEVs at s is $q^s \doteq \sum_{r \in R} q^{rs}$.

$$\begin{aligned} \min_{f, q \geq 0} \quad & \sum_{a \in \mathcal{E}'} \int_0^{\sum_{r \in R} \sum_{s \in S} f_a^{rs}} tt_a(u) du \\ & + \frac{1}{\beta_1} \sum_{r \in R} \sum_{s \in S} q^{rs} (\ln q^{rs} - 1 + \beta_2 \rho^s - \beta_0^s) \end{aligned} \quad (4a)$$

$$\text{s.t. } (\tau^{rs}) \quad Af^{rs} = q^{rs} E^{rs}, \forall r \in R, s \in S, \quad (4b)$$

$$\sum_{s \in S} q^{rs} = d^r, \forall r \in R \quad (4c)$$

Notice that the AEVs associated with each rs will have heterogeneous SOC and travel schedule. We can estimate the distribution of $(SOC_r^{arr}, SOC_r^{dep})$ and (T_r^{arr}, T_r^{dep}) from activity-based travel survey (e.g., [30]) assuming AEVs are fully charged before they start the first trip. These distributions can be further used to estimate the distribution of $(SOC_{rs}^{arr}, SOC_{rs}^{dep})$ and $(T_{rs}^{arr}, T_{rs}^{dep})$ considering the time and energy consumed from r to s . We group the AEVs arriving at a different charging facility s into different types \mathcal{V}_s based on their travel schedule and battery characteristics (e.g., battery capacity, maximum charging/discharging power). We denote the distribution of SOC_v^{arr} and SOC_v^{dep} as probability density function $f_v^{arr}(\cdot)$ and $f_v^{dep}(\cdot)$, respectively, and we denote the flow of each AEV type as q_v (so that $\sum_{v \in \mathcal{V}_s} q_v = q^s$). We can calculate the aggregate charging demand $(SOC_v^{arr}, SOC_v^{dep})$ as in (5). The aggregate charging demand and the corresponding travel plan will serve as input parameters for the charging and battery degradation models, as we discuss in the next section.

$$SOC_v^{arr} = q_v \int_0^{SOC^{max}} u f_v^{arr}(u) du, \forall v \in \mathcal{V}_s \quad (5a)$$

$$SOC_v^{dep} = q_v \int_0^{SOC^{max}} u f_v^{dep}(u) du, \forall v \in \mathcal{V}_s \quad (5b)$$

1 C. AEV Charging and Battery Degradation

We assume that each AEV is equipped with V2G technologies, which enable two-way power flow between vehicles and the grid. Based on the aggregated charging demand $(SOC_v^{arr}, SOC_v^{dep})$ and travel schedule (T_v^{arr}, T_v^{dep}) , $\forall v \in \mathcal{V}_{n,t}$ in Section II-B, we formulate the charging behaviors of AEVs in (6) and (7). For each node n at time t , there can be different AEVs ($v \in \mathcal{V}_{n,t}$) connected, with the SOC constraints described in (6), where (6a) specifies the SOC transition over time; (6b) constrains the feasible range; and (6c) and (6d) define the arrival and minimum departure SOC.

$$soc_{v,t} = soc_{v,t-1} + (\eta_v^{chg} p_{v,t}^{chg} - p_{v,t}^{dsg}) \Delta T, \forall v, t \in [T_v^{arr}, T_v^{dep}] \quad (6a)$$

$$SOC_v^{min} \leq soc_{v,t} \leq SOC_v^{max}, \forall v, t \in [T_v^{arr}, T_v^{dep}] \quad (6b)$$

$$soc_{v,t} = SOC_v^{arr}, \forall v, t = T_v^{arr} \quad (6c)$$

$$soc_{v,t} \geq SOC_v^{dep}, \forall v, t = T_v^{dep} \quad (6d)$$

For a given type of AEV, charging/discharging rates are constrained by its battery technology and charging infrastructure, which are depicted in constraint (7).

$$0 \leq p_{v,t}^{cha} \leq P_v^{\max,cha}, \forall v, t \in [T_v^{\text{arr}}, T_v^{\text{dep}}] \quad (7a)$$

$$0 \leq p_{v,t}^{dsg} \leq P_v^{\max,dsg}, \forall v, t \in [T_v^{\text{arr}}, T_v^{\text{dep}}] \quad (7b)$$

Battery degradation due to frequent charging/discharging is one of the main factors preventing EV owners from participating in V2G programs [31]. Battery cost was still about \$200~\$400 per kWh in 2015, which remains a large portion (25%~50%) of the total AEV cost [32]. Meanwhile, the average life of a typical lithium-ion battery is only about 4500 full cycles [33] and can degrade quickly with frequent charging/discharging. Although battery cost is not the direct cost for the DSO, they typically need to reimburse AEV drivers for participating in V2G programs. In this paper, we assume that the DSO will compensate AEV drivers an amount equal to their battery degradation cost. Battery degradation can be divided into shelf degradation (calendar fade) and cycle degradation [34]. Shelf degradation corresponds to the normal corrosion process, which is independent of its charging and discharging behavior. Here we assume the shelf degradation to be linear over time. Cycle degradation occurs during the charging and discharging process, which is affected by factors such as temperature, charging/discharging rate, and depth of discharge. Different battery degradation models have been proposed for different applications, such as EV bidding problems [35], EV schedule problems [36], and energy storage operation [37]. In this paper, we follow the Ah-throughput counting model [38], as shown in (8). Equation (8a) implies that the capacity degradation, $cap_{v,t}^{\text{loss}}$, is proportional to the energy charged and discharged. Generally, the battery is considered to reach its end of life when its normalized capacity decreases to a specific level, for example, 80%. Thus the cycle degradation percentage, $d_{v,t}^{\text{cycle}}$, can be calculated by (8b). For a given period, the battery degradation is set as the larger one between the shelf degradation and cycle degradation (8c). The degradation cost $c_{v,t}^{\text{deg}}$ is the product of battery cost and the degradation (8d). Here the battery cost is the difference between the replacement cost C_v^{rep} and the residual value (scrap value) C_v^{res} of battery packs.

$$cap_{v,t}^{\text{loss}} = \zeta_v(p_{v,t}^{cha} + p_{v,t}^{dsg})\Delta T \quad (8a)$$

$$d_{v,t}^{\text{cycle}} = \frac{cap_{v,t}^{\text{loss}}}{1 - cap_v^{\text{end}}} \quad (8b)$$

$$d_{v,t} = \max\{d_{v,t}^{\text{cycle}}, d_{v,t}^{\text{shelf}}\} \quad (8c)$$

$$c_{v,t}^{\text{deg}} = d_{v,t}(C_v^{\text{rep}} - C_v^{\text{res}})cap_v \quad (8d)$$

- Considering the degradation cost and the existence of charging and discharging flow, the objective function (1a) and flow balance (1b and 1c) will be modified as (9) and (10a and 10b).

$$\begin{aligned} & \sum_{t \in \mathcal{T}} \sum_{nm \in \mathcal{E}} [\Delta T \cdot R_{nm} \cdot (p_{nm,t}^2 + q_{nm,t}^2) \cdot C^e + z_{nm,t} C^{sw}] \\ & + \sum_{t \in \mathcal{T}} \sum_{n \in \mathcal{N}} \sum_{v \in \mathcal{V}_n} c_{v,t}^{\text{deg}} \end{aligned} \quad (9)$$

$$\begin{aligned} \sum_{m:mn \in \mathcal{E}} p_{mn,t} - \sum_{m:nm \in \mathcal{E}} p_{nm,t} &= P_{n,t}^l + \sum_{v \in \mathcal{V}_n} (p_{v,t}^{cha} - p_{v,t}^{dsg}), \\ \forall n \in \mathcal{N}/\mathcal{N}^s, t \end{aligned} \quad (10a)$$

$$\begin{aligned} \sum_{m:mn \in \mathcal{E}} q_{mn,t} - \sum_{m:nm \in \mathcal{E}} q_{nm,t} &= Q_{n,t}^l + \sum_{v \in \mathcal{V}_n} [F(PF_v^{cha})p_{v,t}^{cha} \\ &- F(PF_v^{dsg})p_{v,t}^{dsg}], \forall n \in \mathcal{N}/\mathcal{N}^s, t \end{aligned} \quad (10b)$$

The optimization problem for DDNR with AEVs is summarized in (11), which is a mixed integer quadratic programming (QP) problem.

$$\min_{\substack{x,y,p,q \\ p^{cha}, p^{dsg}}} \quad (9) \quad (11a)$$

$$\text{s.t.} \quad (1d \sim 1n), (2 \sim 8), (10) \quad (11b)$$

We close this section with two remarks: first, the decentralized nature of AEVs should not be confused with the centralized operation of distribution network. We highlight the decentralized nature of AEVs to emphasize the decisions (facility location choice and route choice) about AEVs are independently made based on system conditions, such as service cost and traffic, but the whole distribution system is still centralized controlled by a DSO; second, we note that the scope of this study is to minimize total system cost (including grid operational cost and consumers cost), so we do not model pricing and transaction of electricity and V2G services. If only the benefits of utility companies are of interest, it may be necessary to model the V2G service costs and the temporal/spatial variation of electricity prices, and to capture revenue changes due to shifting of charging. This is beyond the scope of this study and will be left for the future.

III. NUMERICAL EXPERIMENTS AND ANALYSES

We test our models on a test system overlaying the IEEE 33-node test feeder [11] (see Figure 2a) and Sioux Falls transportation network [39] (see Figure 2b). The lines marked in red or dashed in Figure 2a are equipped with remote switches and the nodes marked in green in Figure 2b are candidate parking and charging locations with PV panels³. The correspondence of nodes number between Figures 2a and 2b are shown in Table I. Although we use only a small test network, we note that the QP formulation of DNR problem have been evidenced for larger systems applications, compared to quadratically constrained and second-order cone formulation [25]. The DDNR model is implemented in C++ using IBM's Concert Technology Library 2.9 and CPLEX 12.7 MIQP solver, and the CDA model is solved using the interior point method, Ipopt [40]. The optimality gap is set to be 0.01%.

In our case studies, we simulated a period of 24 hours. We randomly assign 32 load nodes as residential, commercial, and industrial. The hourly variations of different types of loads are derived from [19]. The cost of switching operation is assumed to be \$500 per switch, considering the possible

³Note that AEVs can choose to charge at the same locations, i.e. $r = s$

TABLE I
NODE CORRESPONDENCE

Transportation Node	1	2	4	5	10	11	13	14	15	19	20	21
Power Node	1	4	6	11	13	16	19	2	23	25	27	32

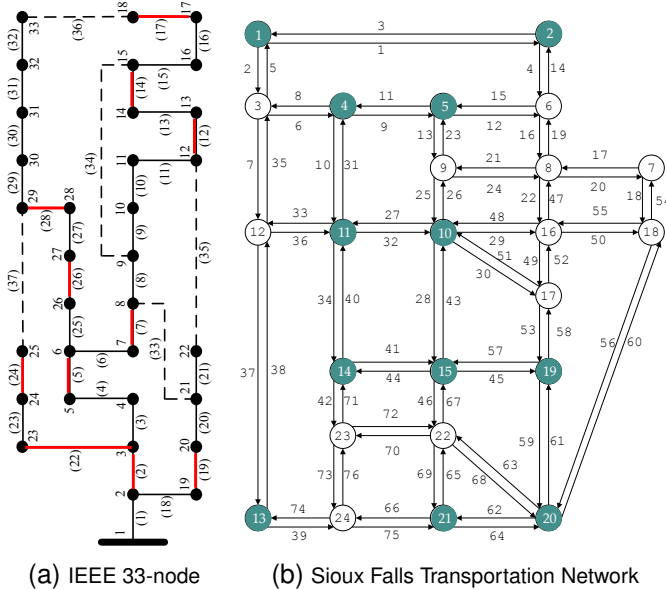


Fig. 2. Test Networks

risk of system instability; energy cost for line losses is \$0.08/kwh [41]. We use the travel patterns of conventional vehicles as a proxy for AEVs and sample travel trajectories from the 2011 Raw Data of Travel Behavior released by the Atlanta Regional Commission (ARC) [30]. After arriving at a certain destination, AEVs could make additional trips to parking/charging locations as long as they can come back with enough battery to fulfill the following trips. In this paper, we only consider parking/charging after arriving at home or work because the majority of AEVs dwelling time happens at these two locations. In total, there are 1,200 AEVs⁴, evenly distributed to 12 green nodes. Each AEV has a battery capacity of 24kWh and requires at least 95% of battery charged at departure. We note that this work focuses on the feasibility of integration of AEVs charging management and DDNR. Further research is necessary to quantify the sensitivities of these parameters in different system settings.

The impacts of integrating DDNR, controllable charging (CC), and V2G technologies on system costs can be seen in Figure 3. Notice that because the system is infeasible without CC technologies, we only report the numerical results for four cases: (a) CC only; (b) CC and V2G; (c) CC and DDNR; and (d) CC, V2G, and DDNR. The infeasibility of the system without CC technologies indicates two things: first, CC is effective in peak load shaving and power quality control, which is consistent with existing literature (see, e.g.,

⁴We assume there is a population of 50,500 for the scale of our network. With an average car ownership of 0.792 cars/person ([30]), 1,200 AEVs is 3% of the total number of cars. The reason we adopt a relatively low AEV penetration rate is because the current system will not be feasible with high AEV penetration without upgrade.

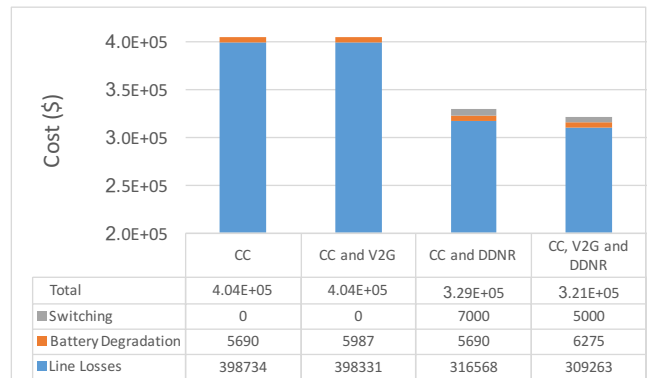


Fig. 3. System Cost with Different Technologies

[42]); on the other hand, distribution system upgrades may be necessary to accommodate more charging load in the distribution network. Comparing cases (a) and (b), adding V2G does not reduce the system cost if only CC is available, let alone additional capital cost for installing bi-directional chargers. Although V2G has been shown to be effective in terms of providing energy and ancillary services to the power system [43], the ineffectiveness of V2G in reducing line losses can be attributed to two competing factors. (1) its peak load shaving effect makes power flow smoother over time. Given the total daily flow fixed, more homogeneous flow leads to less system losses due to the quadratic relationship between flow and line loss (see (9)). (2) V2G will increase the total flow passing through feeders due to their charging and discharging activities, which increases total line losses.⁵ Comparing cases (c) and (d), adding V2G to a system with CC and DDNR, the total system cost can be further reduced by 2.5%. These results show that DDNR complements the V2G technologies in terms of reducing line losses⁶ because the increased feeder flow due to V2G may result in smaller line losses due to the flexibility of topology reconfiguration and flow path changing. Second, DDNR is the most effective technology for reducing total system cost. This can be seen when comparing cases (a) and (c), or cases (b) and (d). Adding DDNR to the distribution network can reduce the total system cost by nearly 20% compared to the cases without DDNR. Third, comparing cases (c) and (d), the additional battery degradation cost due to V2G is only 7.5% of the total system cost reduction, which means it is economically feasible for utility companies to compensate the AEVs owners in order to encourage them to participate in the V2G services.

The key benefit of AEVs over EVs is spatial flexibility of their charging. To investigate how different connecting locations of AEVs will impact the value of V2G to the overall system cost, we conduct 200 simulations, each with

⁵To rule out the impacts of restricting power flow direction on our numerical results, we relaxed the flow direction constraints in Eq. (1f) ~ (1i) and compare cases (a) and (b). We find that the optimal solutions and total system cost are identical to the results shown in Table 5, which indicates that given the assumed relatively low level of AEV penetration, allowing reversed flow will not increase the effectiveness of V2G on line losses.

⁶In addition, [44] has shown that topology reconfiguration complement smart charging strategies to improve voltage profiles with electric vehicles.

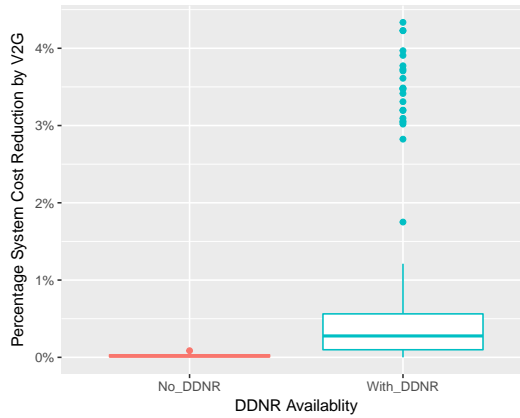


Fig. 4. Random Simulation of AEVs Connecting Locations

randomly assigned AEVs connecting locations. The results are summarized in Figure 4. Notice that the y-axis in Figure 4 is the additional benefits V2G can provide for two scenarios: no DDNR and with DDNR. We find that (1) V2G has much higher value in terms of reducing system costs when DDNR is available, which confirms the observation from Figure 3; and (2) the locations of AEVs are critical when DDNR technology is available, because we can see that certain AEVs connecting locations (i.e., green dots in Figure 4) will make V2G much more valuable for reducing system costs. Location flexibility is one of the key reasons AEVs could provide greater benefits to the system than EVs. Notice that this study only proposes a unifying framework to incorporate the decision making of distribution network operator and AEVs. In the future, it may be beneficial to further investigate how to precisely quantify the benefits of AEVs over EVs.

Although DDNR is receiving increasing attention, frequently switching on/off is not desirable for DSO due to the concerns of switching transient, which may not only reduce power quality and cause short-term outages, but also threaten distribution network stability because of inrush current and difficulties related to relay system coordination. We compare the reconfiguration frequencies between cases (c) and (d), and results are shown in Figure 5. Allowing V2G in the distribution network will create two competing effects on reconfiguration frequency: on one hand, V2G desires more adaptive network topology so that power flow from AEVs can be supplied to more nodes; on the other hand, if we are able to smooth the load by leveraging AEV charging/discharging flexibility, the system will need less reconfiguration. In this study, we only investigate the synthesis of these two effects. As Figure 5 shows, without V2G, the system needs to reconfigure 7 times with 14 switching actions per day; with V2G, reconfiguration frequency decreases to 5 times with 10 switching actions, a reduction of about 28%. These results suggest that for this test example, the benefits from load flexibility of AEVs outweigh the desirability of adaptive network topology.

Next, we investigate the effectiveness of V2G and DDNR on reducing the system operational cost with different PV output variance. The variance of the solar output is measured by the fluctuation over a day. For example, Figure 6 shows

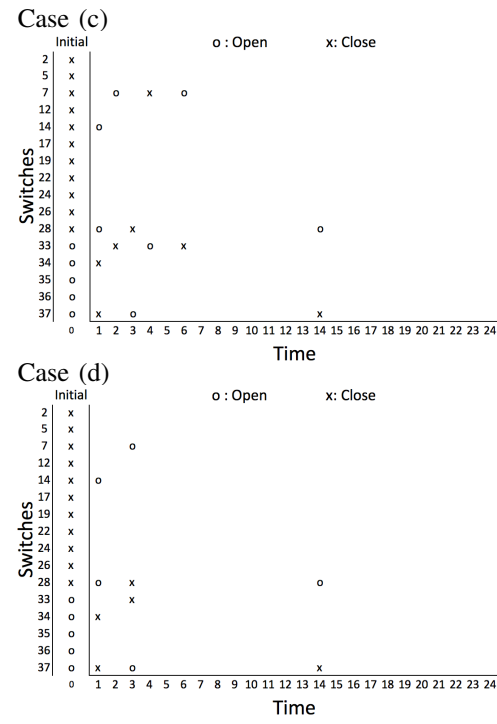


Fig. 5. Switching Actions over Time

a sample PV output for different variance levels. In this case, “20%” means that PV output sequentially increases, and then decreases, from the base level by 20%. Moreover, we scale the total PV outputs in a day up or down to guarantee the total PV outputs are identical across different cases in Figure 6. The system cost reduction percentage for different technologies combinations with respect to the case with only CC are shown in Table II. For example, -20.845% in the cell of “CC, V2G & DDNR” and “0%” means that if we add both V2G and DDNR technology to the system, the total operation cost will decrease by 20.845% at 0% PV output variance level, compared to the case when the system only has CC technology. As shown in Table II, the relative cost reduction percentage are monotonic increasing with higher PV variance if we only add V2G technology. This result suggests that V2G is more effective at reducing system cost when the system load fluctuates more, although the benefits are very limited in our numerical settings. The reason is that V2G provides more capability to smooth the load over time than CC. With the network topology and the total load fixed, smoother power flow over time leads to lower total system line losses. On the other hand, adding DDNR to the system does not have the same monotonic increasing benefits with PV variance, because DDNR has two competing effects: DDNR will be more effective when the system has load variance because the power can go through the most efficient paths by DDNR in order to reduce the line losses; but more PV output variance may lead to higher switching frequency, which increase the system operation cost. The marginal benefits of V2G increase from about 0.019% ~ 0.056% (row 1) to about 2% (compare rows 2 and 3) when DDNR already exists in the system. Similarly, the marginal benefits of DDNR increase from about

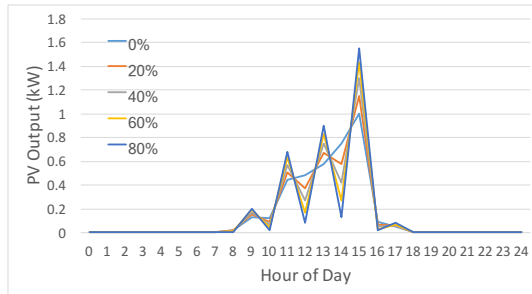


Fig. 6. Sample PV Output for Different Variance Levels

TABLE II
TOTAL COST-SAVING PERCENTAGE FOR DIFFERENT TECHNOLOGIES

PV Variance	0%	20%	40%	60%	80%
CC & V2G	-0.019%	-0.019%	-0.022%	-0.029%	-0.056%
CC & DDNR	-18.878%	-18.584%	-19.042%	-18.912%	-18.998%
CC, V2G & DDNR	-20.845%	-20.838%	-20.865%	-20.846%	-20.235%

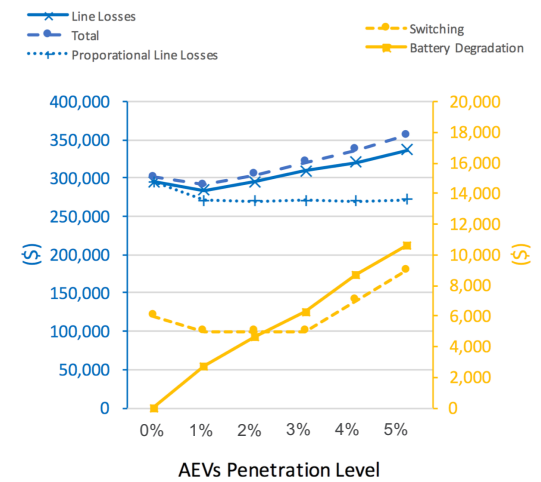


Fig. 7. Impact of Different AEV Penetration Levels

IV. CONCLUSION

We propose a MIQP model to investigate the potential benefits of coordinating charging/discharging actions of AEVs with DDNR considering AEV daily travel patterns, battery degradation costs and decentralized behavior of AEVs. Testing our model on a test system overlaying the IEEE 33-node test feeder and Sioux Falls transportation network, we find that AEVs with controllable charging are necessary to guarantee the feasibility of operating the distribution network. In addition, we find that DDNR technologies complement V2G well in terms of minimizing the total system cost, even considering the extra battery degradation costs associated with V2G services. As a side benefit, the switching actions will decrease slightly following the coordination with AEVs. Varying the solar output fluctuation levels, we find that V2G is more effective with larger solar output fluctuations, while the effectiveness of DDNR is nonlinear with the fluctuation levels. Our numerical results also show an optimal level of AEVs that could minimize the total system cost.

This work can be extended in several directions. From the modeling perspective, we adopted a simplified DistFlow model. Investigating other alternatives to the DistFlow model, such as formulating DNR as second-order cone programming, may generate more accurate descriptions of power flow. Second, our current model could be extended to consider the stochastic nature of the renewable generation, load demand, and AEVs spatial and temporal availability. In addition, we only focus on how to operate the distribution network based on aggregate SOC information at each node in this study. Future research may investigate how to allocate the aggregated charging/discharging strategies to each individual AEV or to AEV categories. In addition, we propose a modeling framework that incorporates a traffic model including the AEVs utilities and choices, based on which incentive design can be further studied. It would also be interesting to conduct more extensive sensitivity analysis, including battery degradation parameters, travel/charging patterns, cost parameters, and other factors.

1 19% (row 2) to 21% (compare rows 1 and 3).

2 Finally, we compare the impacts of different levels of AEV
3 penetration on system cost. We consider six AEV penetration
4 levels, ranging from 0% to 5%. We assume that all the AEVs
5 participate in V2G services and DDNR is available to the
6 system. From Figure 7, we can see that the majority of
7 the system cost comes from line losses regardless of AEV
8 levels. With increasing AEV penetration, the total system cost
9 and the line losses decrease first and then go up. This is
10 the tradeoff between two effects of AEVs: connecting more
11 AEVs to the distribution network will increase the electricity
12 demand, but this will make the load more flexible at the
13 same time. At low levels of AEV penetration (under 1%),
14 the “load flexibility” effect dominates. However, later on, the
15 negative effect of increasing demand outweigh the benefits,
16 which leads to a system cost increase. The proportional line
17 losses⁷ will decrease at low AEV penetration but keep stable
18 after 11%. This indicates that under 5% AEV penetration,
19 increasing charging demand does not increase the unit line
20 losses. For switching cost, when there is no AEVs (0%),
21 the system needs more frequent switching actions (12 times)
22 due to lack of load flexibility; as AEVs increase from 1% to
23 3%, switching actions decrease to 10 occurrences because of
24 the increasing load flexibility and not significantly congested
25 network; as AEVs increase over 4%, the system requires more
26 switching actions to facilitate the operation of a congested
27 distribution network. These observations indicate that for the
28 current distribution network, a low level of AEVs is the most
29 beneficial. Accommodating more AEVs may require system
30 upgrade in order to achieve system functionality and efficiency.
31 Battery degradation costs are almost linear as AEV penetration
32 increase, indicating that no significantly different discharging
33 activities occur for different AEV penetration levels.

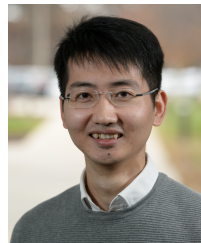
⁷We define proportional line losses as the line losses associated with the original electricity load without AEVs, i.e. the proportional line losses are calculated as the total line losses multiplied by the ratio between the original load and the original AEVs load.

ACKNOWLEDGMENT

The authors acknowledge the U.S. Department of Energy, Office of Energy Efficiency and Renewable Energy for funding the research presented in this paper. The submitted manuscript has been created by UChicago Argonne, LLC, Operator of Argonne National Laboratory (Argonne). Argonne, a U.S. Department of Energy Office of Science laboratory, is operated under Contract No. DE AC02-06CH11357.

REFERENCES

- [1] R. Bradley, "Tesla autopilot, the electric-vehicle maker sent its cars a software update that suddenly made autonomous driving a reality," *MIT Technology Review*, 2016.
- [2] J. Francfort, B. Bennett, R. Carlson, T. Garretson, L. Gourley, D. Karner, and M. Kirkpatrick, "Plug-in electric vehicle and infrastructure analysis," Idaho National Laboratory, Tech. Rep., 2015.
- [3] V. Pimenta, A. Quilliot, H. Toussaint, and D. Vigo, "Models and algorithms for reliability-oriented dial-a-ride with autonomous electric vehicles," *European Journal of Operational Research*, vol. 257, no. 2, pp. 601–613, 2017.
- [4] J. Hernandez-Aceituno, R. Arnay, J. Toledo, and L. Acosta, "Using kinect on an autonomous vehicle for outdoors obstacle detection," *IEEE Sensors Journal*, vol. 16, no. 10, pp. 3603–3610, 2016.
- [5] G. Franz and W. Lucia, "A receding horizon control strategy for autonomous vehicles in dynamic environments," *IEEE Transactions on Control Systems Technology*, vol. 24, no. 2, pp. 695–702, 2016.
- [6] T.-T. Han and S. S. Ge, "Styled-velocity flocking of autonomous vehicles: a systematic design," *IEEE Transactions on Automatic Control*, vol. 60, no. 8, 2015.
- [7] E. Uhlemann, "Autonomous vehicles are connecting...[connected vehicles]," *IEEE Vehicular Technology Magazine*, vol. 10, no. 2, pp. 22–25, 2015.
- [8] A. Lam, J. James, Y. Hou, and V. O. K. Li, "Coordinated autonomous vehicle parking for vehicle-to-grid services: Formulation and distributed algorithm," *IEEE Transactions on Smart Grid*, 2017.
- [9] A. C. Melhorn, K. McKenna, A. Keane, D. Flynn, and A. Dimitrovski, "Autonomous plug and play electric vehicle charging scenarios including reactive power provision: a probabilistic load flow analysis," *IET Generation, Transmission & Distribution*, vol. 11, no. 3, pp. 768–775, 2017.
- [10] C. Peng, J. Zou, and L. Lian, "Dispatching strategies of electric vehicles participating in frequency regulation on power grid: A review," *Renewable and Sustainable Energy Reviews*, vol. 68, pp. 147–152, 2017.
- [11] M. E. Baran and F. F. Wu, "Network reconfiguration in distribution systems for loss reduction and load balancing," *IEEE Transactions on Power Delivery*, vol. 4, no. 2, pp. 1401–1407, 1989.
- [12] M. R. Dorostkar-Ghamsari, M. Fotuhi-Firuzabad, M. Lehtonen, and A. Safdarian, "Value of distribution network reconfiguration in presence of renewable energy resources," *IEEE Transactions on Power Systems*, vol. 31, no. 3, pp. 1879–1888, 2016.
- [13] R. A. Jabr, R. Singh, and B. C. Pal, "Minimum loss network reconfiguration using mixed-integer convex programming," *IEEE Transactions on Power Systems*, vol. 27, no. 2, pp. 1106–1115, 2012.
- [14] S. Lei, J. Wang, C. Chen, and Y. Hou, "Mobile emergency generator pre-positioning and real-time allocation for resilient response to natural disasters," *IEEE Transactions on Smart Grid*, vol. PP, no. 99, pp. 1–1, 2016.
- [15] A. R. Malekpour, T. Niknam, A. Pahwa, and A. K. Fard, "Multi-objective stochastic distribution feeder reconfiguration in systems with wind power generators and fuel cells using the point estimate method," *IEEE Transactions on Power Systems*, vol. 28, no. 2, pp. 1483–1492, 2013.
- [16] K. Chen, W. Wu, B. Zhang, S. Djokic, and G. P. Harrison, "A method to evaluate total supply capability of distribution systems considering network reconfiguration and daily load curves," *IEEE Transactions on Power Systems*, vol. 31, no. 3, pp. 2096–2104, 2016.
- [17] E. Lopez, H. Opazo, L. Garcia, and P. Bastard, "Online reconfiguration considering variability demand: applications to real networks," *IEEE Transactions on Power Systems*, vol. 19, no. 1, pp. 549–553, 2004.
- [18] S. Chen, W. Hu, and Z. Chen, "Comprehensive cost minimization in distribution networks using segmented-time feeder reconfiguration and reactive power control of distributed generators," *IEEE Transactions on Power Systems*, vol. 31, no. 2, pp. 983–993, 2016.
- [19] M. R. Dorostkar-Ghamsari, M. Fotuhi-Firuzabad, M. Lehtonen, and A. Safdarian, "Value of distribution network reconfiguration in presence of renewable energy resources," *IEEE Transactions on Power Systems*, vol. 31, no. 3, pp. 1879–1888, 2016.
- [20] F. Capitanescu, L. F. Ochoa, H. Margossian, and N. D. Hatziargyriou, "Assessing the potential of network reconfiguration to improve distributed generation hosting capacity in active distribution systems," *IEEE Transactions on Power Systems*, vol. 30, no. 1, pp. 346–356, 2015.
- [21] C. Lueken, P. M. S. Carvalho, and J. Apt, "Distribution grid reconfiguration reduces power losses and helps integrate renewables," *Energy Policy*, vol. 48, pp. 260–273, 2012.
- [22] Z. Guo, S. Lei, Y. Wang, Z. Zhou, and Y. Zhou, "Dynamic distribution network reconfiguration considering travel behaviors and battery degradation of electric vehicles," in *2017 IEEE Power and Energy Society General Meeting (PESGM)*, July 2017, pp. 1–5.
- [23] D. Zhang, Z. Fu, and L. Zhang, *Electric Power Systems Research*, vol. 77, no. 5, pp. 685–694, 2007.
- [24] H. Haghifat and B. Zeng, "Distribution system reconfiguration under uncertain load and renewable generation," *IEEE Transactions on Power Systems*, vol. 31, no. 4, pp. 2666–2675, 2016.
- [25] J. A. Taylor and F. S. Hover, "Convex models of distribution system reconfiguration," *IEEE Transactions on Power Systems*, vol. 27, no. 3, pp. 1407–1413, 2012.
- [26] D. McFadden, "Modeling the choice of residential location," *Transportation Research Record*, no. 673, 1978.
- [27] Y. Sheffi, "Urban transportation networks," 1985.
- [28] Z. Guo, J. Deride, and Y. Fan, "Infrastructure planning for fast charging stations in a competitive market," *Transportation Research Part C: Emerging Technologies*, vol. 68, pp. 215–227, 2016.
- [29] J. G. Wardrop, "Some theoretical aspects of road traffic research," in *ICE Proceedings: Engineering Divisions*, vol. 1. Thomas Telford, Conference Proceedings, pp. 325–362.
- [30] P. NuStats, "Regional travel survey: final report," *Atlanta Regional Commission, Atlanta*, 2011.
- [31] H. Farzin, M. Fotuhi-Firuzabad, and M. Moeini-Aghajaei, "A practical scheme to involve degradation cost of lithium-ion batteries in vehicle-to-grid applications," *IEEE Transactions on Sustainable Energy*, vol. 7, no. 4, pp. 1730–1738, 2016.
- [32] T. Randall, "Heres how electric cars will cause the next oil crisis," 2016. [Online]. Available: <http://www.bloomberg.com/features/2016-ev-oil-crisis/>
- [33] B. Dunn, H. Kamath, and J.-M. Tarascon, "Electrical energy storage for the grid: a battery of choices," *Science*, vol. 334, no. 6058, pp. 928–935, 2011.
- [34] K. Smith, E. Wood, S. Santhanagopalan, G.-H. Kim, Y. Shi, and A. Pesaran, "Predictive models of li-ion battery lifetime," in *IEEE Conference on Reliability Science for Advanced Materials and Devices, Golden, Colorado*, 2014, Conference Proceedings.
- [35] E. Yao, V. W. Wong, and R. Schober, "Robust frequency regulation capacity scheduling algorithm for electric vehicles," 2015.
- [36] D. R. Melo, A. Trippe, H. B. Gooi, and T. Massier, "Robust electric vehicle aggregation for ancillary service provision considering battery aging," *IEEE Transactions on Smart Grid*, 2016.
- [37] Y. Wang, Z. Zhou, A. Botterud, K. Zhang, and Q. Ding, "Stochastic coordinated operation of wind and battery energy storage system considering battery degradation," *Journal of Modern Power Systems and Clean Energy*, vol. 4, no. 4, pp. 581–592, 2016.
- [38] S. B. Peterson, J. Apt, and J. Whitacre, "Lithium-ion battery cell degradation resulting from realistic vehicle and vehicle-to-grid utilization," *Journal of Power Sources*, vol. 195, no. 8, pp. 2385–2392, 2010.
- [39] L. J. Leblanc, "An algorithm for the discrete network design problem," *Transportation Science*, vol. 9, no. 3, pp. 183–199, 1975.
- [40] A. Wächter and L. Biegler, "On the implementation of an interior-point filter line-search algorithm for large-scale nonlinear programming," *Mathematical programming*, vol. 106, pp. 25–57, 2006.
- [41] Q. Zhou, D. Shirmohammadi, and W. H. E. Liu, "Distribution feeder reconfiguration for operation cost reduction," *IEEE Transactions on Power Systems*, vol. 12, no. 2, pp. 730–735, May 1997.
- [42] G. Zhang, S. T. Tan, and G. G. Wang, "Real-time smart charging of electric vehicles for demand charge reduction at non-residential sites," *IEEE Transactions on Smart Grid*, vol. 9, no. 5, pp. 4027–4037, 2018.
- [43] E. Sortomme and M. A. El-Sharkawi, "Optimal scheduling of vehicle-to-grid energy and ancillary services," *IEEE Transactions on Smart Grid*, vol. 3, no. 1, pp. 351–359, 2012.
- [44] F. Ding and M. J. Mousavi, "On per-phase topology control and switching in emerging distribution systems," *IEEE Transactions on Power Delivery*, vol. 33, no. 5, pp. 2373–2383, 2018.



Zhaomiao Guo received the B.S. degree in civil engineering from Tsinghua University, Beijing, China, in 2010, the M.S. degree in transportation engineering from the University of California, Berkeley, CA, USA, in 2011, and both the M.S. degree in agricultural and resources economics and the Ph.D. degree in transportation engineering from the University of California, Davis, CA, USA, in 2015 and 2016, respectively. He is currently an assistant professor in the Department of Civil, Environmental, and Construction Engineering (with joint appointment in the Resilient, Intelligent and Sustainable Energy Systems (RISES) cluster) at the University of Central Florida, Orlando, FL, USA. His research centers around modeling and computational strategies for intelligent and resilient critical infrastructure systems, with applications in transportation and energy systems.



Zhi Zhou (M09) received the B.Eng. and M.Eng. degrees in computer science from Wuhan University, Wuhan, China, in 2001 and 2004, respectively, and the Ph.D. degree in decision sciences and engineering systems from Rensselaer Polytechnic Institute, Troy, NY, USA, in 2010. He is currently a Principal Computational Scientist with the Energy Systems Division, Argonne National Laboratory, Lemont, IL, USA. His research interests include agent-based modeling and simulation, stochastic optimization, statistical forecasting, electricity markets, and renewable energy.



Yan Zhou received the B.Eng. degrees in Automotive Engineering from Wuhan University of Technology, Wuhan, China, in 2003, and M.S. the Ph.D. degree in Transportation Engineering from Clemson University, Clemson, SC, USA in 2008 and 2010 respectively. She is currently a group leader and principal scientist in the Energy Systems Division, Argonne National Laboratory, Lemont, IL, USA. Her research interests include energy assessment of vehicle and fuel technologies, as well as advanced fueling infrastructure modeling and deployment.